

Article

RETRACTED: Dual Solutions in a Boundary Layer Flow of a Power Law Fluid over a Moving Permeable Flat Plate with Thermal Radiation, Viscous Dissipation and Heat Generation/Absorption

Aftab Ahmed ¹, Javed I. Siddique ^{2,*} and Muhammad Sagheer ¹

¹ Department of Mathematics, Capital University of Science and Technology, Islamabad 44000, Pakistan; 680aftab@gmail.com (A.A.); sagheer@cust.edu.pk (M.S.)

² Department of Mathematics, Penn State University—York Campus, York, PA 17403-3326, USA

* Correspondence: jis15@psu.edu; Tel.: +1-717-771-4171

Received: 26 November 2017; Accepted: 5 January 2018; Published: 9 January 2018

Abstract: The aim of the present study is to investigate the combined effects of the thermal radiation, viscous dissipation, suction/injection and internal heat generation/absorption on the boundary layer flow of a non-Newtonian power law fluid over a semi infinite permeable flat plate moving in parallel or reversely to a free stream. The resulting system of partial differential equations (PDEs) is first transformed into a system of coupled nonlinear ordinary differential equations (ODEs) which are then solved numerically by using the shooting technique. It is found that the dual solutions exist when the flat plate and the free stream move in the opposite directions. Dimensionless boundary layer velocity and temperature distributions are plotted and discussed for various values of the emerging physical parameters. Finally, the tables of the relevant boundary derivatives are presented for some values of the governing physical parameters.

Keywords: moving plate; power law fluid; viscous dissipation; thermal radiation; suction/injection; heat generation/absorption

1. Introduction

The pioneering work on the boundary layer flow of a viscous incompressible fluid over a stationary flat plate with uniform fluid velocity was due to Blasius [1] in 1908. Following this, many authors [2–6] investigated the Blasius flow problem by considering various flow situations and boundary conditions. Different from the Blasius flow problem, the problem of boundary layer flow and heat transfer over a continuous flat plate moving in parallel or reversely to the free stream was discussed by a number of researchers [7–10] and reported that the dual solutions exist in the case when the plate and the free stream move in the opposite directions. The mathematical analysis of the dual solutions of the boundary layer flow over the moving surfaces has a practical impact in the engineering scenario. It gives the possibility to determine the most realistic, stable and physically acceptable solutions. Weidman et al. [11] established that the upper branch or the first solution is stable and physically more meaningful than the lower branch or the second solution, which nevertheless highlights some interesting mathematical features of the differential equations.

Instead of considering the plate velocity U_w and the free stream velocity U_∞ separately [12,13], Afzal et al. [14] obtained a single set of boundary conditions by employing the idea of composite velocity $U = U_w + U_\infty$, irrespective of whether $U_w > U_\infty$ or $U_w < U_\infty$. They have thus given a formulation which eliminates the need of considering U_w or U_∞ as a reference velocity in a flow problem. Moreover, the Blasius and Sakiadis flow problems can be recovered as a special case when $U_w = 0$ and $U_\infty = 0$, respectively.

The study of non-Newtonian fluids has gained considerable importance over the years due to their increasing industrial and technological demands. One such non-Newtonian fluid model is the Ostwald-de Waele or the power law model which is commonly used to predict the dynamics of shear thinning and shear thickening fluids and can reproduce the results for the Newtonian fluid case as well. Such fluids are widely encountered in engineering and industry in the form of polymers, paints, suspensions, rubber and bio-fluids. Schowalter [15] first studied the boundary layer flow of the non-Newtonian power law fluid and established the condition for the existence of similarity solution. Later on, Mahmoud [16] and Kannan et al. [17] investigated the boundary layer flow and heat transfer of the power law fluid over a moving flat plate but only for the case when the flat plate and the ambient fluid move in the same direction. Deswita et al. [18] reported the dual solutions for the power law fluid flow with suction and injection effects and neglected the heat transfer effects. Apart from these studies, power law fluid modeling under different flow situations can be found in the literature [19–21] and the references therein.

Thermal radiation can be used to achieve the desired heat transfer rate along with the temperature distribution in the boundary layer region. This phenomenon has many applications in engineering such as power generation systems, nuclear reactors and liquid metal fluids to name a few. Bataller [22] studied the Blasius flow problem in the presence of thermal radiation and reported that as the thermal radiation parameter increases, a diminution in the thermal radiation's effect occurs. The Sakiadis flow problem for the Newtonian fluid case with the linearized Rosseland approximation for the thermal radiation was investigated numerically by Cortell [23]. Recently, Pantokratoras et al. [24,25] extended the work of Bataller and Cortell by taking into account the nonlinear approximation of the thermal radiation. These studies were confined to the situation when either the flat plate was stationary or the surface and the free stream move in the same direction. Ishak [26] generalized this idea and studied the radiation effect on the flow and heat transfer over a flat surface by considering the case in which the flat plate and the free stream move in the same as well as opposite directions thus giving the dual solutions of the boundary layer velocity and temperature profiles.

Viscous dissipation generates an appreciable amount of temperature in a system and gives the rate at which the mechanical energy is transformed into the heat energy in a viscous fluid per unit volume. This phenomenon plays an important role in natural convection in various devices which are subjected to very low temperature, high gravitational field or that operate at high rotational speed [27]. It is important to note that the viscous dissipation effect becomes significant for fluids with high values of the dynamic viscosity. Kishan and Reddy [28] investigated the magnetohydrodynamics (MHD) effect on the power-law fluid past a continuously moving porous flat plate in the presence of viscous dissipation, heat flux and suction/injection. Cooney et al. [29] discussed the effect of viscous dissipation and thermal radiation on the unsteady MHD free convection flow over an infinite heated vertical plate in a porous medium with time dependent suction.

Motivated by the above mentioned studies and by following the work of Ishak [26], the aim of the present investigation is to carry out numerical computations to give dual solutions for the steady, two dimensional laminar boundary layer flow of a power law fluid over a permeable semi infinite moving flat plate with combined effects of the thermal radiation, viscous dissipation, prescribed surface temperature and internal heat generation or absorption. This study differentiates from the previous related studies in the sense that we employ here the idea of composite velocity introduced by Afzal et al. [14] and give dual solutions of the boundary layer velocity and temperature distributions. To the best of our knowledge, this case is not already reported in the literature. This article is organized as follows: In Section 2, we present the mathematical formulation of the problem. Section 3 contains the numerical procedure for solving the governing system of differential equations. Section 4 deals with the results and discussion followed by the dual solutions in Section 5. Finally, the conclusions are furnished in Section 6.

2. Flow Analysis

To develop the model, we consider the steady, forced convective laminar boundary layer flow over a permeable semi infinite flat plate moving with constant velocity U_w in the same or opposite to the direction of the free stream velocity U_∞ . We place the fluid in a two dimensional environment where x -axis is taken parallel to the surface, while y -axis extends upwards, normal to the surface as shown in Figure 1. The fluid behavior is described by the power law model for which the shear stress τ is defined as [20,30]

$$\tau = \mu \left| \frac{\partial u}{\partial y} \right|^{n-1} \frac{\partial u}{\partial y} \tag{1}$$

where μ is the consistency index for non-Newtonian viscosity and n is the power law index which subdivides fluids into Newtonian ($n = 1$), shear thinning ($n < 1$) and shear thickening ($n > 1$).

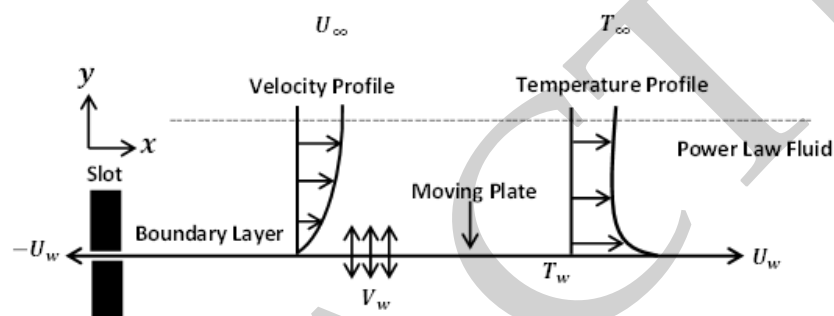


Figure 1. Physical model and coordinate system.

Keeping in view Equation (1), we invoke the conservation of mass, momentum and energy to describe the fluid flow and heat transfer in the boundary layer by the following set of partial differential equations (PDEs) [16,30]

$$\frac{\partial u}{\partial x} + \frac{\partial v}{\partial y} = 0 \tag{2}$$

$$u \frac{\partial u}{\partial x} + v \frac{\partial u}{\partial y} = \frac{\mu}{\rho} \frac{\partial}{\partial y} \left(\left| \frac{\partial u}{\partial y} \right|^{n-1} \frac{\partial u}{\partial y} \right) \tag{3}$$

$$u \frac{\partial T}{\partial x} + v \frac{\partial T}{\partial y} = \frac{\kappa}{\rho c_p} \frac{\partial^2 T}{\partial y^2} - \frac{1}{\rho c_p} \frac{\partial q_r}{\partial y} + \frac{\mu}{\rho c_p} \left| \frac{\partial u}{\partial y} \right|^{n+1} + \frac{Q_0(T - T_\infty)}{\rho c_p} \tag{4}$$

where u and v are the velocity components in the x and y directions, respectively, ρ the fluid density, T the fluid temperature, κ the thermal conductivity, c_p the specific heat capacity of the participating fluid at constant pressure, q_r the radiative heat flux, Q_0 the heat generation or absorption coefficient, T_∞ the free stream temperature. Equations (2)–(4) are subjected to the following boundary conditions:

$$u = U_w, \quad v = V_w, \quad T = T_w \quad \text{at} \quad y = 0 \tag{5}$$

$$u \rightarrow U_\infty, \quad T \rightarrow T_\infty \quad \text{as} \quad y \rightarrow \infty \tag{6}$$

where $T_w = T_\infty + Ax^r$ is the prescribed surface temperature in which r is the power law exponent and A is a constant [31]. Note that $r > 0$ represents the case when the surface temperature varies directly with r while $r < 0$ means the surface temperature varies inversely with the exponent r . T_∞ is the free stream temperature which is assumed to be constant with $T_w > T_\infty$. Moreover, V_w is the velocity of the suction ($V_w < 0$) or injection ($V_w > 0$) and $U = U_w + U_\infty$ is defined to be the composite velocity [14]

in which U_w is the plate and U_∞ is the free stream velocity. Employing the Rosseland approximation for radiation [26], we write

$$q_r = \frac{-4\sigma}{3\kappa^*} \frac{\partial T^4}{\partial y} = \frac{-4\sigma}{3\kappa^*} \frac{\partial}{\partial y} (4T_\infty^3 T - 3T_\infty^4) = \frac{-16\sigma T_\infty^3}{3\kappa^*} \frac{\partial T}{\partial y} \tag{7}$$

where σ is the Stefan-Boltzman constant and κ^* is the mean absorption co-efficient. Using Equation (7) into (4), we get

$$u \frac{\partial T}{\partial x} + v \frac{\partial T}{\partial y} = \frac{1}{\rho c_p} \left(\kappa + \frac{16\sigma T_\infty^3}{3\kappa^*} \right) \frac{\partial^2 T}{\partial y^2} + \frac{\mu}{\rho c_p} \left| \frac{\partial u}{\partial y} \right|^{n+1} + \frac{Q_0(T - T_\infty)}{\rho c_p} \tag{8}$$

We now introduce a stream function $\psi = \psi(x, y)$ and write the velocity components u and v as

$$u = \frac{\partial \psi}{\partial y}, \quad v = -\frac{\partial \psi}{\partial x} \tag{9}$$

Using these velocity components in Equations (3) and (8), we obtain

$$\frac{\partial \psi}{\partial y} \frac{\partial^2 \psi}{\partial x \partial y} - \frac{\partial \psi}{\partial x} \frac{\partial^2 \psi}{\partial y^2} = \frac{\mu}{\rho} \frac{\partial}{\partial y} \left(\left| \frac{\partial^2 \psi}{\partial y^2} \right|^{n-1} \frac{\partial^2 \psi}{\partial y^2} \right) \tag{10}$$

$$\frac{\partial \psi}{\partial y} \frac{\partial T}{\partial x} - \frac{\partial \psi}{\partial x} \frac{\partial T}{\partial y} = \left(\kappa + \frac{16\sigma T_\infty^3}{3\kappa^*} \right) \frac{\partial^2 T}{\partial y^2} + \frac{\mu}{\rho c_p} \left| \frac{\partial^2 \psi}{\partial y^2} \right|^{n+1} + \frac{Q_0(T - T_\infty)}{\rho c_p} \tag{11}$$

Note that the continuity Equation (2) is satisfied identically by virtue of Equation (9). Boundary conditions (5) and (6) can be written in view of (9) as

$$\frac{\partial \psi}{\partial y} = U_w, \quad \frac{\partial \psi}{\partial x} = -V_w, \quad T = T_w \quad \text{at} \quad y = 0 \tag{12}$$

$$\frac{\partial \psi}{\partial y} \rightarrow U_\infty, \quad T \rightarrow T_\infty \quad \text{as} \quad y \rightarrow \infty \tag{13}$$

We use the following non-dimensional variables [16]

$$\eta = y \left(\frac{U^2 - n}{\nu x} \right)^{1/n+1}, \quad \psi(\eta) = (\nu x U^{2n-1})^{1/n+1} f(\eta), \quad \theta(\eta) = \frac{T - T_\infty}{T_w - T_\infty} \tag{14}$$

to reduce the PDEs (10) and (11) to the corresponding ODEs as

$$n |f''|^{n-1} f''' + \frac{1}{n+1} f f'' = 0 \tag{15}$$

$$\frac{3R+4}{3RPr} \theta'' + \frac{1}{n+1} f \theta' + Ec |f''|^{n+1} + \gamma \theta - r f' \theta = 0 \tag{16}$$

where prime denotes the derivative with respect to the similarity variable η , $\nu = \frac{\mu}{\rho}$ represents the kinematic viscosity, f is the dimensionless stream function, θ the dimensionless temperature, Pr the generalized Prandtl number, R the radiation parameter, Ec the Eckert number, γ the local heat generation ($\gamma > 0$) or absorption ($\gamma < 0$) parameter and r the power law surface temperature exponent, which are further defined as [16,26]

$$Pr = \frac{\rho c_p}{\kappa} \left(\frac{U^3}{x} \right)^{\frac{n-1}{n+1}} \left(\frac{\mu}{\rho} \right)^{\frac{2}{n+1}}, \quad R = \frac{\kappa k^*}{4\sigma T_\infty^3}, \quad Ec = \frac{U^2}{c_p(T_w - T_\infty)}, \quad \gamma = \frac{x Q_0}{U \rho c_p} \tag{17}$$

Note that in equation (16), $\frac{1}{R} \rightarrow 0$ implies that the thermal radiation effect is negligible. By using the relations for η and ψ given by Equation (14), velocity components u and v in Equation (9) can be written as

$$u = Uf'(\eta), \quad v = \frac{-U}{(n+1)x} \left(\frac{\mu x}{\rho U^{2-n}} \right)^{\frac{1}{n+1}} (f(\eta) - \eta f'(\eta)) \tag{18}$$

and the mass transfer velocity V_w takes the form

$$V_w = \frac{-U}{(n+1)x} \left(\frac{\mu x}{\rho U^{2-n}} \right)^{\frac{1}{n+1}} S \tag{19}$$

Finally, the boundary conditions (12) and (13) are transformed to

$$f'(\eta) = \epsilon, \quad f(\eta) = S, \quad \theta(\eta) = 1 \quad \text{at} \quad \eta = 0 \tag{20}$$

$$f'(\eta) \rightarrow 1 - \epsilon, \quad \theta(\eta) \rightarrow 0 \quad \text{as} \quad \eta \rightarrow \infty \tag{21}$$

where $\epsilon = \frac{U_w}{U}$ is the plate velocity ratio parameter, $S = f(0)$ is the local suction or injection parameter with suction if $S > 0$, injection if $S < 0$ and impermeable plate when $S = 0$. We term the flow situation as assisting or aiding flow when the flat plate and the power law fluid move in the same direction (i.e., $0 < \epsilon < 1$) and opposing flow in the case when they move in the opposite directions (i.e., $\epsilon < 0$ or $\epsilon > 1$). The quantities of practical interest are the skin friction coefficient C_f and the local Nusselt number Nu_x , which are defined as

$$C_f = \frac{2\tau_w}{\rho U^2}, \quad Nu_x = \frac{xq_w}{\kappa(T_w - T_\infty)} \tag{22}$$

where the surface shear stress τ_w and the surface heat flux q_w are given by

$$\tau_w = \left[\mu \left(\frac{\partial u}{\partial y} \right)^n \right]_{y=0}, \quad q_w = -\kappa \left(\frac{\partial T}{\partial y} \right)_{y=0} \tag{23}$$

In terms of the non-dimensional quantities, we can write the last two equations as

$$\frac{1}{2} C_f (Re_x)^{\frac{1}{n+1}} = [f''(0)]^n, \quad Nu_x (Re_x)^{\frac{-1}{n+1}} = -\theta'(0) \tag{24}$$

where $Re_x = \frac{\rho x^n U^{2-n}}{\mu}$ is the local generalized Reynolds number [16].

3. Numerical Procedure

In this section, we briefly outline the shooting method in the context of the problem under consideration. In particular, we use this method to solve the nonlinear two point boundary value problem (15)–(16) and (20)–(21). This requires the conversion of the governing boundary value problem to the corresponding initial value problem. For this we set

$$f' = p, \quad p' = q, \quad q' = \frac{-1}{n(n+1)} f q |q|^{1-n} \tag{25}$$

$$\theta' = z, \quad z' = \frac{-3RPr}{3R+4} \left[\frac{1}{n+1} f z + Ec |q|^{n+1} + \gamma \theta - rp \theta \right] \tag{26}$$

along with the boundary conditions

$$p(\eta) = \epsilon, \quad f(\eta) = S, \quad \theta(\eta) = 1, \quad \text{at} \quad \eta = 0 \tag{27}$$

$$p(\eta) \rightarrow 1 - \epsilon, \quad \theta(\eta) \rightarrow 0 \quad \text{as} \quad \eta \rightarrow \infty \tag{28}$$

In order to apply the shooting method, we need to choose a suitable finite value of the right end of the domain, say η_∞ in place of ∞ , and carry out numerical computations so that the far field boundary conditions $f'(\eta_\infty) = 1 - \epsilon$ and $\theta(\eta_\infty) = 0$ are asymptotically satisfied. In this study, we choose $\eta_\infty = 18$ which suffices to achieve the accuracy up to 10^{-6} . Moreover, the shooting method requires initial guesses for $f''(0)$ and $\theta'(0)$ i.e., $q(0)$ and $z(0)$ respectively, and through the Newton method, we modify each guess until we arrive at an appropriate solution of the problem under consideration [32]. For the verification of these solutions, we compare our results as a special case with the existing literature [26] and find the results to be in an excellent agreement.

4. Results and Discussion

In this section, we first present a table for the skin friction coefficient $[f''(0)]^n$ for the power law fluid for various values of the governing parameters and then furnish a comparison table for the local Nusselt number $-\theta'(0)$ with the existing literature followed by the discussion on the graphs of the boundary layer velocity and temperature to highlight the effects of various emerging physical parameters.

Table 1 presents the numerical values of the skin friction coefficient $[f''(0)]^n$ for the power law fluid for different values of the suction/injection parameter S and the velocity ratio parameter ϵ . It can be seen that the skin friction at the surface wall decrease as the power law index n , the suction/injection parameter S and the velocity ratio parameter ϵ , increase. Moreover, due to less viscosity and rapid motion of shear thinning fluids at the surface wall, shear thinning fluids experience greater skin friction at the wall as compared to shear thickening fluids. When the free stream velocity is twice the plate velocity then the skin friction at the flat plate is zero whereas when both the free stream and the plate velocities are the same, the skin friction is negative.

Table 1. Numerical values of the skin friction coefficient $[f''(0)]^n$ for various values of n, S and ϵ .

n	S	ϵ	$[f''(0)]^n$	
0.7	0	0	0.452398	0.452399
1.0	0	0	0.332057	0.332060
1.3	0	0	0.256248	0.256249
1.0	-0.5	1.0	-0.309749	-0.309750
1.0	0	1.0	-0.443748	-0.443750
1.0	0.5	1.0	-0.604013	-0.604018
1.0	0	0	0.332057	0.332060
1.0	0	0.5	0	0
1.0	0	1.0	-0.443748	-0.443750

In Table 2, we present a comparison of the numerical values of the local Nusselt number $-\theta'(0)$ with the results of Ishak [26] for the Newtonian fluid case and in the absence of suction/injection, heat generation/absorption and viscous dissipation. An excellent agreement is observed for the upper as well as lower branch solutions.

Figure 2 presents the effect of the velocity ratio parameter ϵ and the power law index n on the non-dimensional boundary layer velocity $f'(\eta)$ for a fixed value of the suction parameter S . It is observed from this graph that near the flat plate fluid velocity increases by increasing the velocity ratio parameter for both Newtonian and non-Newtonian fluids whereas opposite trend is noted for larger values of η . In the boundary layer region due to the decreased velocity gradient at the wall, the participating fluid experiences less resistance which results in an increase of the fluid velocity in this region. On the other hand, for a fixed value of ϵ , it is found that the fluid velocity increases by increasing the power law index n for the large distance from the flat plate. In particular, when the parameter ϵ is non-negative, shear thinning fluids exhibit greater fluid velocity near the flat plate in comparison to shear thickening fluids whereas, for positive ϵ , fluid velocity is increased for shear thickening fluids. Moreover, steady-state is achieved earlier for the shear thickening fluids in comparison to the shear

thinning fluids. Influence of the suction/injection parameter S on the power law fluid velocity $f'(\eta)$ for a positive value of the velocity ratio parameter ϵ is presented in Figure 3. It is found from this graph that the power law fluid velocity increases by increasing the suction/injection parameter for a given distance from the flat plate. By sucking the particles of the fluid adjacent to the porous flat plate, velocity boundary layer decreases and consequently the power law fluid velocity increases. It can also be seen that for various values of the parameters n and S , the far field boundary condition is reached asymptotically (i.e., the velocity gradient at large distance from the flat plate is zero).

Table 2. A comparison of values of $-\theta'(0)$ for various Pr, R and ϵ when $n = 1, S = 0, Ec = 0, \gamma = 0, r = 0$.

Pr	R	ϵ	Ishak [26]		Present Study	
			Upper Branch	Lower Branch	Upper Branch	Lower Branch
0.7	10	-0.5	0.192108	0.102369	0.192108	0.102369
0.7	10	-0.4	0.222545	0.065939	0.222544	0.065943
0.7	10	-0.3	0.242122	0.040663	0.242122	0.040663
0.7	10	-0.2	0.257162	0.020581	0.257161	0.020582
0.7	10	-0.1	0.269469	0.005075	0.269468	0.004991
5	0.7	0	0.401067	-	0.401066	-
5	1	0	0.432419	-	0.432418	-
5	3	0	0.509212	-	0.509212	-
5	7	0	0.543692	-	0.543691	-
5	10	0	0.552813	-	0.552812	-
5	50	0	0.571588	-	0.571587	-
5	100	0	0.574116	-	0.574115	-
5	1000	0	0.576430	-	0.576429	-
5.5	0.6	1	0.621122	-	0.621122	-
5.5	5.5	1	1.078558	-	1.078558	-
5.5	7	1	1.104468	-	1.104467	-
5.5	10	1	1.134987	-	1.134987	-
5.5	50	1	1.198589	-	1.198588	-
5.5	100	1	1.207234	-	1.207233	-
5.5	10000	1	1.216050	-	1.212048	-

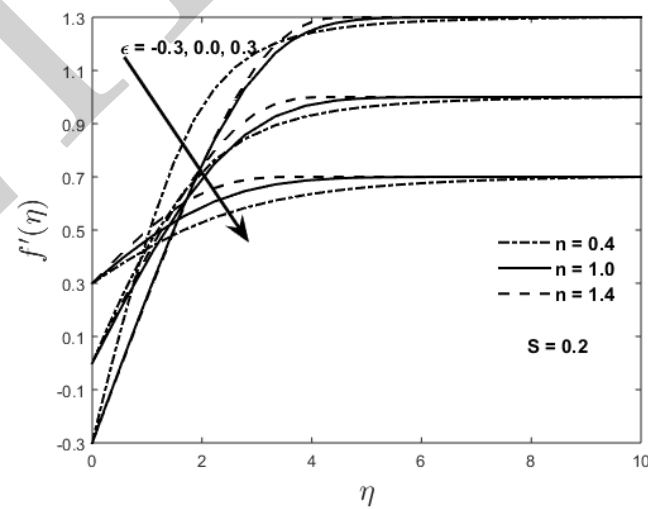


Figure 2. Velocity profiles for various values of ϵ and n .

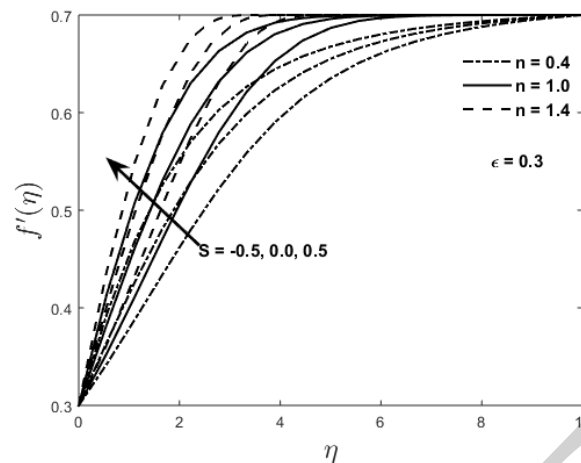


Figure 3. Velocity profiles for various values of S and n .

In Figure 4, we present the effect of the suction/injection parameter S on the power law fluid temperature $\theta(\eta)$ for fixed values of the other parameters. It is evident from this graph that as the parameter S increases, the power law fluid temperature decreases for a given distance from the permeable flat plate. This effect is consistent with a number of previous studies where a non-Newtonian power law fluid model was considered [16,17]. In fact, suction brings the fluid closer to the surface causing an increase in the heat transfer rate which reduces the thermal boundary layer thickness and hence the power law fluid temperature decreases by increasing the parameter S . Indeed, larger suction leads to faster cooling of the plate, and this phenomenon plays an important role in many engineering applications. This graph also explains that the fluid temperature $\theta(\eta)$ increases by increasing the power law index n for a fixed value of the parameter S . An increase in the value of the power law index n means that the fluid is more viscous, and due to the high viscosity, the fluid temperature drops off slowly. The effect of varying the radiation parameter R on the power law fluid temperature $\theta(\eta)$ for the plate ratio parameter $\epsilon = 0.3$ and Prandtl number $Pr = 0.7$, is depicted in Figure 5. Increasing the value of the radiation parameter R means, the release of more heat energy from the flow region, which results in a decrease in the power law fluid temperature $\theta(\eta)$ for a given distance from the moving plate which is shown in Figure 5. Effect of the power law index n on the fluid temperature is more prominent for low values of the radiation parameter. On the other hand, for very large values of the radiation parameter, no significant difference in the temperature for both the Newtonian and the non-Newtonian fluids is observed.

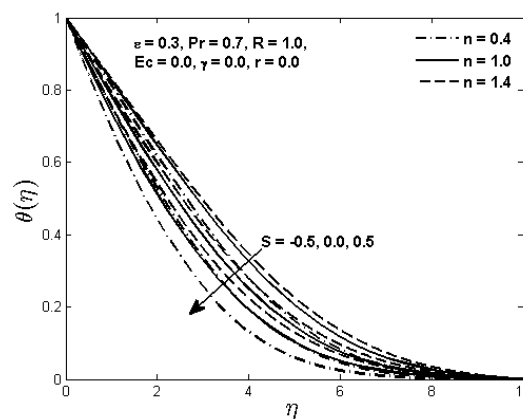


Figure 4. Temperature profiles for various values of S and n .

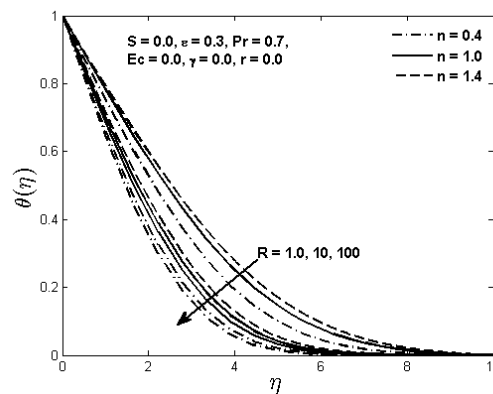


Figure 5. Temperature profiles for various values of R and n .

Influence of the Eckert number Ec (which expresses the relationship between the kinetic energy and enthalpy difference characterizes the heat dissipation in the system) and heat generation/absorption parameter γ on dimensionless power law fluid temperature $\theta(\eta)$ in the boundary layer region is illustrated in Figures 6 and 7, respectively, for the case when the flat plate and the free stream move in the same direction. It is evident from Figure 6 that the fluid temperature increases as the Eckert number increases for a given distance from the plate. This is because of the fact that an increase in the Eckert number leads to the cooling of the plate which in turn transfers the heat to the fluid and thus the fluid temperature rises in the boundary layer region. It can also be observed from this graph that the effect of the Eckert number is more profound in shear thinning fluids as compared to the shear thickening fluids. From Figure 7, we observe that the dimensionless power law fluid temperature $\theta(\eta)$ increases by increasing the heat generation/absorption parameter γ for a positive value of the velocity ratio parameter ϵ . Effect of the power law index n is more prominent in case of the heat generation ($\gamma > 0$) than the heat absorption ($\gamma < 0$). Moreover, in the case of heat generation, maximum value of the fluid temperature occurs at the fluid layer adjacent to the plate for both the Newtonian as well as non-Newtonian fluids. The thermal boundary layer thickness and hence the fluid temperature decreases in case of the heat absorption whereas an opposite trend is noted for the heat generation case.

Figures 8 and 9 display the effect of the power law surface temperature parameter r on the fluid temperature $\theta(\eta)$ in the boundary layer region when the flat surface moves in parallel (i.e., $\epsilon > 0$) or reversely (i.e., $\epsilon < 0$) to the free stream. Both graphs show that the temperature for the Newtonian ($n = 1$) as well as the non-Newtonian ($n \neq 1$) fluids decreases as the parameter r increases for a given distance from the flat surface. Moreover, the thermal boundary layer thickness for the assisting flow (i.e., $\epsilon > 0$) is greater than the opposing flow (i.e., $\epsilon < 0$) situation for the power law fluid. It can also be noted from these graphs that the temperature rise is higher in the case of the opposing flow as compared to the assisting flow. Effect of the power law index is more profound for positive values of the prescribed surface temperature parameter r in both graphs. Although, we presented here a single solution of the power law fluid temperature for the situation when the plate and the free stream move in opposite directions (i.e., when $\epsilon < 0$), nevertheless, dual solutions exist in this case and will be discussed in the next section.

Figure 10 illustrates the effect of varying the Prandtl number Pr (which is the ratio of momentum diffusivity to thermal diffusivity) on the temperature distribution in the boundary layer for the case when the velocity ratio parameter $\epsilon > 0$. It is found that the fluid temperature decreases for both the Newtonian and non-Newtonian fluids as the Prandtl number increases. Physically, this corresponds to the situation where the thermal boundary layer thickness is reduced due to an increase in the parameter Pr . In addition, effect of the power law index n is more dominating for larger Prandtl number values as compared to the lower values. In Figure 11, the rate of heat transfer or the local Nusselt number $-\theta'(0)$

is plotted against the radiation parameter R for various values of the Prandtl number Pr and power law index n . This graph highlights three key points of the present research. Firstly, for a fixed Prandtl number and power law index, it is noticed that the rate of heat transfer increases as the radiation parameter increases for a given distance from the flat plate. Secondly, heat transfer rate increases with the increasing values of the Prandtl number. This is because of the fact that higher Prandtl number reduces the thermal boundary layer thickness which in turn decreases the fluid temperature, and then the heat can diffuse faster from the plate to the fluid. Thirdly, due to less viscosity of the shear thinning fluids, heat energy can be transported to the neighboring fluid particles easily, and hence the rate of heat transfer is higher in the shear thinning fluids than the shear thickening fluids. Moreover, effect of the power law index on the local Nusselt number is more dominating for the higher Prandtl numbers.

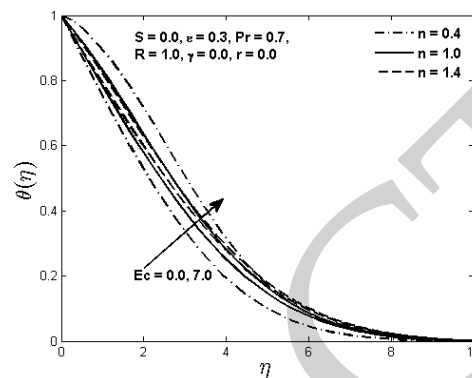


Figure 6. Temperature profiles for various values of Ec and n .

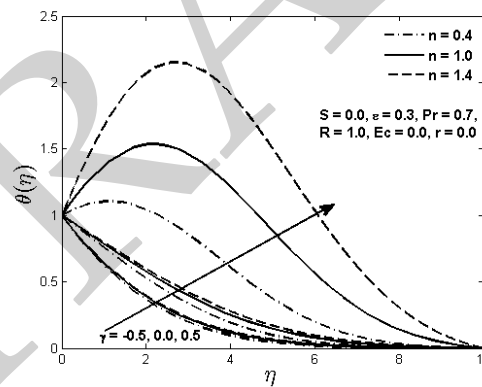


Figure 7. Temperature profiles for various values of γ and n .

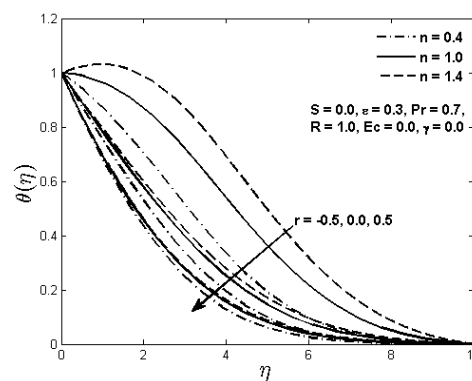


Figure 8. Temperature profiles for various values of r and n when $\epsilon > 0$.

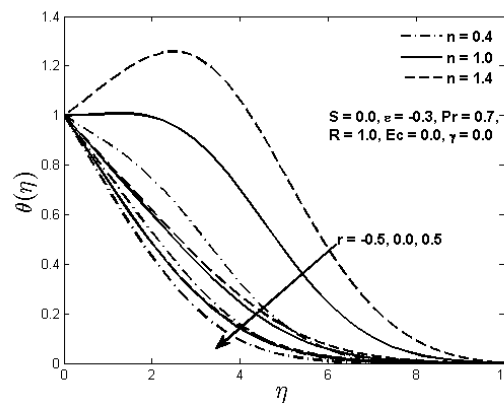


Figure 9. Temperature profiles for various values of r and n when $\epsilon < 0$.

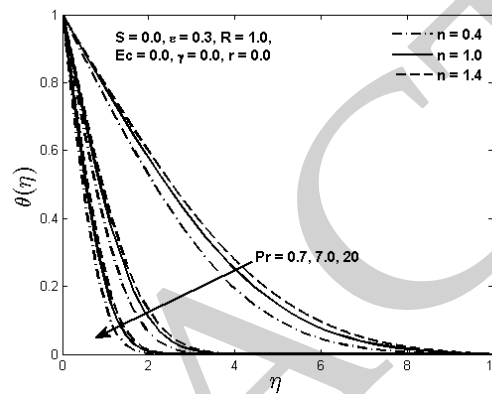


Figure 10. Temperature profiles for various values of Pr and n .

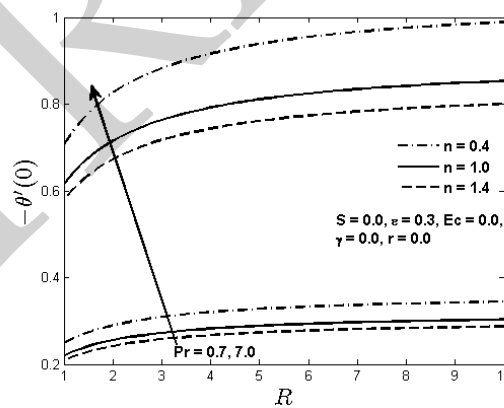


Figure 11. $-\theta'(0)$ vs. R for various values of Pr and n .

5. Dual Solutions

In this section, we present the dual solutions of the boundary layer velocity and temperature profiles by means of the graphs for various values of the governing physical parameters for the opposing flow situation in which the plate and the power law fluid move in the opposite directions. By the dual solutions of a boundary value problem, we mean two different solutions that are obtained under the same conditions by assuming different values of the missing initial conditions. Such solutions despite being graphically different are physically acceptable and satisfy the prescribed boundary conditions. Of the two solutions, one is termed as the first or upper branch solution while the other is

called the second or the lower branch solution of the boundary value problem. From physical point of view, it is important to know that which solution is physically relevant. Unlike the second solution, we expect that the first solution is physically stable and frequently occurs in practice [8,10,11,26]. Based on our numerical computations, we notice that the dual solutions exists for $\epsilon < 0$ and unique solution exist when $\epsilon \geq 0$. In this study, we consider the case when $\epsilon \leq 1$. Note that $\epsilon = 0$ implies $U_w = 0$ (stationary plate) and $\epsilon = 1$ means $U_\infty = 0$ (in the absence of porosity). In the opposing flow scenario, when the plate and the fluid move in opposite directions there exist some critical values denoted by ϵ_c of the velocity ratio parameter ϵ beyond which the boundary layer breaks down and no solution exists.

Figures 12 and 13 present the dual solutions of the fluid velocity $f'(\eta)$ and the temperature $\theta(\eta)$ for the suction/injection parameter S in case of the opposing flow situation, respectively. As the parameter S increases, the fluid velocity increases monotonically for the upper branch solution whilst a reverse behavior is observed for the lower branch solution as shown in Figure 12. Boundary layer thickness for the lower branch solution is found larger than the upper branch solution. It can be also be seen that the right boundary condition is reached asymptotically in both cases and the effect of the parameter S is more profound for the lower branch solution as compared to the upper one. In Figure 13, the fluid temperature is found to decrease with the increasing suction/injection parameter S for the upper branch solution whereas it increases for the lower branch solution. Moreover, the lower branch solution exhibits larger thermal boundary layer thickness than the upper branch solution.

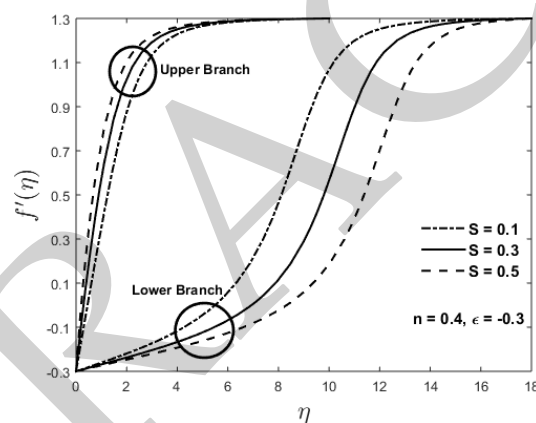


Figure 12. Dual solutions of velocity for various values of S .

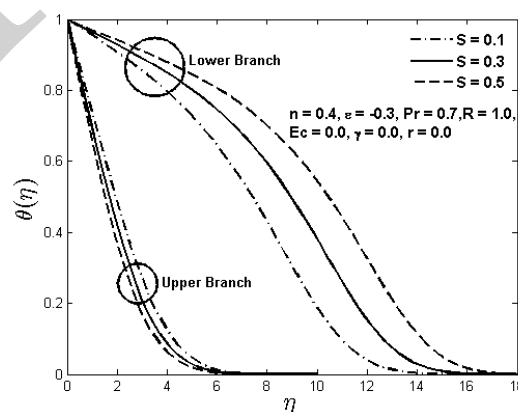


Figure 13. Dual solutions of temperature for various values of S .

Finally, the dual nature of the fluid temperature $\theta(\eta)$ for the Eckert number Ec and the heat generation/absorption parameter γ is presented in Figures 14 and 15, respectively when the other

parameters are held constant. Interestingly, the fluid temperature increases by increasing the Eckert number as well as the heat generation/absorption parameter for the lower and upper branch solution for a given distance from the flat surface. As observed earlier, the thermal boundary layer thickness is higher for the lower branch solution in comparison to the upper branch solution. This fact supports the argument that the upper branch solutions are stable and physically relevant as compared to the lower branch solutions.

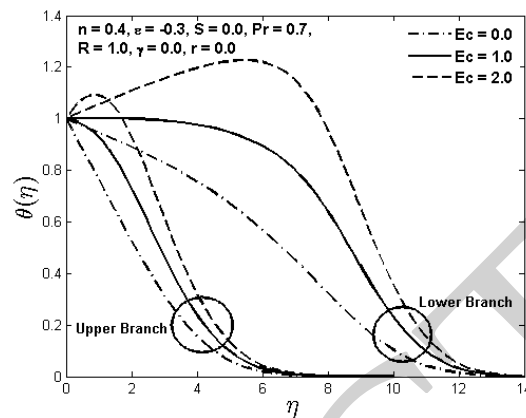


Figure 14. Dual solutions of temperature for various values of E_c .

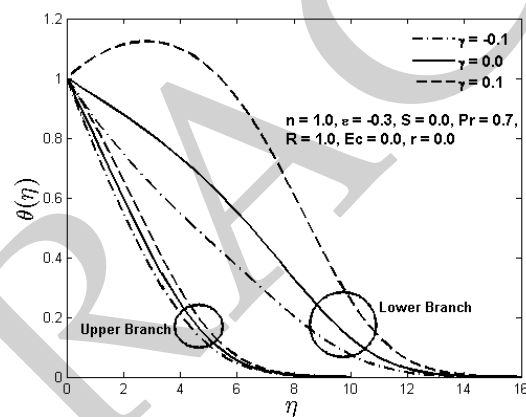


Figure 15. Dual solutions of temperature for various values of γ .

6. Conclusions

We have analyzed the steady state, two-dimensional, boundary layer flow of a power law fluid over a porous moving flat plate in the presence of the thermal radiation, viscous dissipation and internal heat generation or absorption. The governing system of PDEs is transformed to the corresponding system of coupled nonlinear ODEs and subsequently solved using the shooting technique. We discussed the graphs of the nondimensional velocity and temperature profiles for various values of the system parameters along with tables of the relevant boundary derivatives. At the end, we present a summary of our results:

1. Fluid velocity and temperature increase by increasing the power law index.
2. Skin friction at the surface wall decreases by increasing the power law index, suction/injection and velocity ratio parameter.
3. Rate of heat transfer increases by increasing the Prandtl number and the radiation parameter whilst an opposite behavior is observed for the power law index.
4. Power law fluid velocity increases with the suction parameter for the upper branch solution while a reverse effect is noted in case of the lower branch solution. Moreover, an opposite trend of the fluid velocity is seen for the power law fluid temperature with the suction parameter.

5. Power law fluid temperature increases by increasing the Eckert number and the heat generation/absorption parameter for the upper as well as the lower branch solution with more dominating effect in case of the lower branch solution.
6. Fluid temperature decreases for the Newtonian as well as the non-Newtonian fluids by increasing the power law surface temperature parameter for the assisting and opposing flow situations.

The basic features of this model may be incorporated in further studies for different flow situations in complex media. We anticipate that incorporation of additional features such as multidimensional flow, magnetohydrodynamics and slip effects may be considered as a future direction. In addition to this further theoretical and experimental studies may be motivated by our work.

Acknowledgments: Author Javed I. Siddique would like to acknowledge support from Simons Foundation under grant No.281839.

Author Contributions: All the three authors have contributed equally in the preparation of this manuscript.

Conflicts of Interest: The authors declare no conflict of interest.

Nomenclature

u	velocity component in x direction	LT^{-1}
x	horizontal distance	L
μ	dynamic viscosity	$ML^{-1}T^{-1}$
q_w	surface heat flux	MT^{-3}
κ	thermal conductivity of fluid	$MLK^{-1}T^{-3}$
q_r	radiative heat flux	MT^{-3}
c_p	specific heat capacity of fluid	$L^2K^{-1}T^{-2}$
Q_0	heat generation/absorption coefficient	$MK^{-1}T^{-3}$
τ_w	surface shear stress	MLT^{-2}
σ	Stefan-Boltzman constant	$MK^{-4}T^{-3}$
ν	kinematic viscosity	L^2T^{-1}
η	similarity variable	1
$\theta(\eta)$	dimensionless temperature	1
R	radiation parameter	1
γ	heat generation/absorption parameter	1
S	suctionparameter	1
n	power law index	1
C_f	skin friction coefficient	1
v	velocity component in y direction	LT^{-1}
y	vertical distance	L
ρ	fluid density	ML^{-3}
T	fluid temperature	K
T_w	wall temperatue	K
U_w	wall velocity	LT^{-1}
T_∞	free stream temperature	K
U_∞	free stream velocity	LT^{-1}
V_w	velocity of suction/injection	LT^{-1}
κ^*	Mean absorption coefficient	L^{-1}
ψ	stream function	L^2T^{-1}
$f(\eta)$	dimensionless stream function	1
Pr	Prandtl number	1
Ec	Eckert number	1
ϵ	velocity ratio parameter	1
r	power law temperature exponent	1
Re_x	generalized Reynolds number	1
Nu_x	local Nusselt number	1

References

1. Blasius, H. Grenzschichten in Flüssigkeiten mit kleiner Reibung. *Zeitschrift für Angewandte Mathematik und Physik* **1908**, *56*, 1–37.
2. Pohlhausen, E. Der Wärmeaustausch zwischen festen Körpern und Flüssigkeiten mit kleiner Reibung und kleiner Wärmeleitung. *Zeitschrift für Angewandte Mathematik und Mechanik* **1921**, *1*, 121–151.
3. Howarth, L. On the solution of the laminar boundary layer equations. *Proc. R. Soc. Lond. A* **1938**, *164*, 547–579.
4. Wang, L. A new algorithm for solving classical Blasius equation. *Appl. Math. Comput.* **2004**, *157*, 1–9.
5. Bataller, R.C. Radiation effects for the Blasius and Sakiadis flows with a convective surface boundary condition. *Appl. Math. Comput.* **2008**, *206*, 832–840.
6. Cortell, R. Numerical solutions of the classical Blasius flat-plate problem. *Appl. Math. Comput.* **2005**, *170*, 706–710.
7. Sakiadis, B.C. Boundary-layer behavior on continuous solid surfaces boundary-layer equations for two dimensional and axisymmetric flow. *AIChE J.* **1961**, *7*, 26–28.
8. Ishak, A.; Nazar, R.; Pop, I. Flow and heat transfer characteristics on a moving flat plate in a parallel stream with constant surface heat flux. *Heat Mass Transf.* **2009**, *45*, 563–567.
9. Mukhopadhyay, S. Dual solutions in boundary layer flow of a moving fluid over a moving permeable surface in presence of prescribed surface temperature and thermal radiation. *Chin. Phys. B* **2014**, *23*, 014702.
10. Mukhopadhyay, S.; Bhattacharyya, K.; Layek, G.C. Steady boundary layer flow and heat transfer over a porous moving plate in presence of thermal radiation. *Int. J. Heat Mass Transf.* **2011**, *54*, 2751–2757.
11. Weidman, P.D.; Kubitschek, D.G.; Davis, A.M.J. The effect of transpiration on self-similar boundary layer flow over moving surfaces. *Int. J. Eng. Sci.* **2006**, *44*, 730–737.
12. Abdelhafez, T.A. Skin friction and heat transfer on a continuous flat surface moving in a parallel free stream. *Int. J. Heat Mass Transf.* **1985**, *28*, 1234–1237.
13. Chappidi, P.R.; Gunnerson, F.S. Analysis of heat and momentum transport along a moving surface. *Int. J. Heat Mass Transf.* **1989**, *32*, 1383–1386.
14. Afzal, N.; Badaruddin, A.; Elgarvi, A.A. Momentum and transport on a continuous flat surface moving in a parallel stream. *Int. J. Heat Mass Transf.* **1993**, *36*, 3399–3403.
15. Schowalter, W.A. The application of boundary layer theory to power-law pseudo plastic fluid similar solutions. *AIChE J.* **1960**, *6*, 24–28.
16. Mahmoud, M.A.A. Slip velocity effect on a non-Newtonian power-law fluid over a moving permeable surface with heat generation. *Math. Comput. Model.* **2011**, *54*, 1228–1237.
17. Kannan, T.; Moorthy, M.B.K. Effects of variable viscosity on Power-Law fluids over a permeable moving surface with slip velocity in the presence of heat generation and suction. *J. Appl. Fluid Mech.* **2016**, *9*, 2791–2801.
18. Deswita, L.; Ishak, A.; Nazar, R. Power-law fluid flow on a moving wall with suction and injection effects. *Aust. J. Basic Appl. Sci.* **2010**, *4*, 2250–2256.
19. Khan, W.A.; Gorla, R.S.R. Heat and mass transfer in power-law nanofluids over a nonisothermal stretching wall with convective boundary condition. *J. Heat Transf.* **2012**, *134*, 112001–112007.
20. Reddy, B.; Kishan, N.; Rajasekhar, M. MHD boundary layer flow of a non-Newtonian power-law fluid on a moving flat plate. *Adv. Appl. Sci. Res.* **2012**, *3*, 1472–1481.
21. Acrivos, A.; Shah, M.J.; Petersen, E.E. Momentum and heat transfer in laminar boundary layer flows of non-Newtonian fluids past external surfaces. *AIChE J.* **1960**, *6*, 312–317.
22. Bataller, R.C. Radiation effects in the Blasius flow. *Appl. Math. Comput.* **2008**, *198*, 333–338.
23. Cortell, R. A numerical tackling on Sakiadis flow with thermal radiation. *Chin. Phys. Lett.* **2008**, *25*, 1340–1342.
24. Pantokratoras, A.; Fang, T. Blasius flow with non-linear Rosseland thermal radiation. *Meccanica* **2014**, *49*, 1539–1545.
25. Pantokratoras, A.; Fang, T. Sakiadis flow with nonlinear Rosseland thermal radiation. *Phys. Scr.* **2012**, *87*, 015703.
26. Ishak, A. Radiation effects on the flow and heat transfer over a moving plate in a parallel stream. *Chin. Phys. Lett.* **2009**, *26*, 034701.

27. Gebhart, B. Effect of viscous dissipation in natural convection. *J. Fluid Mech.* **1962**, *14*, 225–235.
28. Kishan, N.; Reddy, B.S. MHD effects on non-Newtonian power-law fluid past a continuously moving porous flat plate with heat flux and viscous dissipation. *Int. J. Appl. Mech. Eng.* **2013**, *18*, 425–445.
29. Cookey, C.I.; Ogulu, A.; Omubo-Pepple, V.B. Influence of viscous dissipation and radiation on unsteady MHD free convection flow past an infinite heated vertical plate in a porous medium with time dependent suction. *Int. J. Heat Mass Transf.* **2003**, *46*, 2305–2311.
30. Rao, J.H.; Jeng, D.R.; De Witt, K.J. Momentum and heat transfer in a power law fluid with arbitrary injection/suction at a moving wall. *Int. J. Heat Mass Transf.* **1999**, *42*, 2837–2847.
31. Mukhopadhyay, S.; Golra, R.S.R. Dual solutions for boundary layer flow of moving fluid over a moving surface with power-law surface temperature. *Int. J. Appl. Mech. Eng.* **2013**, *18*, 113–124.
32. Na, T.Y. *Computational Methods in Engineering Boundary Value Problems*; Academic Press: New York, NY, USA, 1979; Volume 145.



© 2018 by the authors. Licensee MDPI, Basel, Switzerland. This article is an open access article distributed under the terms and conditions of the Creative Commons Attribution (CC BY) license (<http://creativecommons.org/licenses/by/4.0/>).